

# Dynamics of first-order quantum phase transitions in extended Bose-Hubbard model: From density wave to superfluid and vice-versa

Keita Shimizu<sup>1</sup>, Takahiro Hirano<sup>1</sup>, Jonghoon Park<sup>1</sup>, Yoshihito Kuno<sup>2</sup> and Ikuo Ichinose<sup>1</sup>

<sup>1</sup> Department of Applied Physics, Nagoya Institute of Technology, Nagoya 466-8555, Japan

<sup>2</sup> Department of Physics, Graduate School of Science, Kyoto University, Kyoto 606-8502, Japan

E-mail: k.shimizu.268@nitech.jp

**Abstract.** In this paper, we study the nonequilibrium dynamics of the Bose-Hubbard model with the nearest-neighbor repulsion by using time-dependent Gutzwiller (GW) methods. In particular, we vary the hopping parameters in the Hamiltonian as a function of time, and investigate the dynamics of the system from the density wave (DW) to the superfluid (SF) crossing a first-order phase transition and vice-versa. From the DW to SF, we find scaling laws for the correlation length and vortex density with respect to the quench time. This is a reminiscence of the Kibble-Zurek scaling for continuous phase transitions and contradicts the common expectation. We give a possible explanation for this observation. On the other hand from the SF to DW, the system evolution depends on the initial SF state. When the initial state is the ground-state obtained by the static GW methods, a coexisting state of the SF and DW domains forms after passing through the critical point. Coherence of the SF order parameter is lost as the system evolves. This is a phenomenon similar to the glass transition in classical systems. When the state starts from the SF with small local phase fluctuations, the system obtains a large-size DW-domain structure with thin domain walls.

PACS numbers: 67.85.Hj, 03.75.Kk, 05.30.Rt

*Keywords:* Ultra-cold atomic gases, Bose-Hubbard model, Quantum dynamical phase transition, First-order phase transition, Superfluid, Density wave.

## 1. Introduction

In recent years, dynamics of quantum-many body systems is one of the most actively studied subjects in physics. Process in which a system approach to an equilibrium is of fundamental interests, and also evolution of system under a quench has attracted many physicists. Nowadays, ultra-cold atomic gas systems play a very important role for the study on these subjects because of their versatility, controllability and observability [1]. Theoretical ideas proposed to understand transient phenomena are to be tested by experiments on ultra-cold atomic systems. This is one of examples of so-called quantum simulations [2, 3, 4, 5].

For the second-order thermal phase transition, time-evolution of systems under a change in temperature has been studied extensively so far. From the view point of cosmology, Kibble [6, 7] claimed that the phase transitions lead to disparate local choices of the broken symmetry state and as a result, topological defects called cosmic strings are generated. Later, Zurek [8, 9, 10] pointed out that a similar phenomenon is realized in laboratory experiments on the condensed matter systems like the superfluid (SF) of  $^4\text{He}$ . After the above seminal works, many theoretical and experimental studies on the Kibble-Zurek (KZ) mechanism have appeared [11]. Concerning to experiments on Bose-condensed ultra-cold atomic gases, the correlation length of the SF and the rate of topological defect formation were measured and the KZ scaling hypothesis was examined [12, 13].

To study dynamics of quantum many-body systems, the parameters in the Hamiltonian are varied through a quantum phase transition (QPT), i.e., the quantum quench [13, 14, 15, 16, 17, 18, 19, 20, 21, 22, 23, 24, 25, 26], and the system evolution is observed. Experiments on this problem have been already done using the various ultra-cold atomic gases [27, 28, 29, 30, 31, 32]. Among them, works in Refs. [27, 28] questioned the applicability of the KZ scaling theory to the QPT, whereas Refs. [29, 30] concluded that the observed results were in good agreement with the KZ scaling law.

In this paper, we focus on the two-dimensional (2D) Bose-Hubbard model (BHM) [33, 34], which is a canonical model of the bosonic ultra-cold atomic gas systems in an optical lattice. In particular, we add nearest-neighbor (NN) repulsions between atoms. Then, the resultant system is described by an extended Bose-Hubbard model (EBHM). As a result, a parameter region corresponding to the density wave (DW) appears in the ground-state phase diagram, in addition to the Mott insulator and SF. Near the half-filling, there exists a first-order phase transition between the SF and DW [35]. We shall study the quench dynamics of the EBHM on passing across the SF and DW phase boundary. There are only a few works for the dynamical properties of quantum systems at first-order phase transitions under a quench [36, 38, 39], and therefore detailed study on that problem is desired.

This paper is organized as follows. In Sec. 2, we introduce the EBHM and explain the Gutzwiller (GW) methods, which are used in the present work. In Sec. 3, quench dynamics of the first-order phase transition from the DW to SF is studied. Behavior

of SF and DW orders are investigated by solving the Schrödinger equation by means of time-dependent GW (tGW) methods. We focus on the order parameters, correlation length, vortex number, etc, in particular, scaling laws of these quantities with respect to the quench time  $\tau_Q$ . Contrary to the common expectation, we find that scaling laws hold for the correlation length and vortex density. In Sec. 4, we give a possible explanation of the observed results from viewpoint of the SF bubble-nucleation process. We employ a time-dependent Ginzburg-Landau theory and show that scaling laws with small deviations from the KZ scaling hold in the vicinity of a triple point in the phase diagram. Applicability of the GW methods is also discussed there. In Sec. 5, we study the time evolution of the system from the SF to DW crossing the first-order phase transition. We find that even for very slow quench, a genuine DW does not form if we start the time evolution with the ground-state obtained by the static GW methods. Numerical result shows that a coexisting state of the SF and DW appears instead. On the other hand, if SF states with small coherent phase fluctuations are employed as an initial state, the system acquires a DW domain structure of large size with thin domain walls. Section 6 is devoted for conclusion. In appendix, we show the results obtained for the hard-core Bose-Hubbard model, in which the first-order phase transition between the DW and SF exists as in the soft-core system of the present work. We discuss the behavior of the correlation length and vortex density compared to the soft-core case.

## 2. Extended Bose-Hubbard model and slow quench

We consider the EBHM whose Hamiltonian is given by [42],

$$\begin{aligned}
 H_{\text{BH}} = & -J \sum_{\langle i,j \rangle} (a_i^\dagger a_j + \text{H.c.}) + \frac{U}{2} \sum_i n_i (n_i - 1) \\
 & + V \sum_{\langle i,j \rangle} n_i n_j - \mu \sum_i n_i,
 \end{aligned} \tag{1}$$

where  $\langle i, j \rangle$  denotes NN sites of a square lattice,  $a_i^\dagger$  ( $a_i$ ) is the creation (annihilation) operator of boson at site  $i$ ,  $n_i = a_i^\dagger a_i$ , and  $\mu$  is the chemical potential.  $J(> 0)$  and  $U(> 0)$  are the hopping amplitude and the on-site repulsion, respectively. We also add the NN repulsion with the coefficient  $V$ , which plays an important role in the present work.

In this study, we are interested in cases near the half filling, i.e.,  $\rho \equiv \frac{1}{N_s} \sum_i \langle n_i \rangle \approx 1/2$ , where  $N_s$  is the total number of the lattice sites, and we take  $N_s = 64 \times 64$  or  $100 \times 100$  for the practical calculation. We set  $U = 1$  as the energy unit, and time  $t$  is measured in the unit  $\hbar/U$ . We investigated the system in Eq.(1) by using the static GW approximation and show obtained ground-state phase diagram in Fig. 1 for  $V/U = 0.05$ . There exist three phases, i.e., the DW, SF and supersolid (SS) although the area of the SS in the phase diagram is small for  $V/U = 0.05$ . We also show the system energy, particle density and amplitude of the SF order parameter,  $|\Psi| \equiv \frac{1}{N_s} \sum_i |\Psi_i|$ , where  $\Psi_i \equiv \langle a_i \rangle$ , in Fig. 2 for  $\mu/U = 0.1$ . From the results in Fig. 2, it is obvious that the

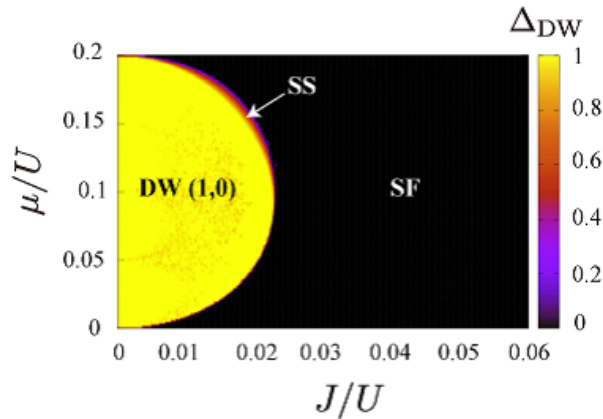


**Figure 1.** Ground-state phase diagram of the extended Bose-Hubbard model for  $V = 0.05$  obtained by the static GW methods. There exist three phases, the density wave (DW), superfluid (SF) and supersolid (SS). Mean particle density  $\rho \approx 1/2$ .

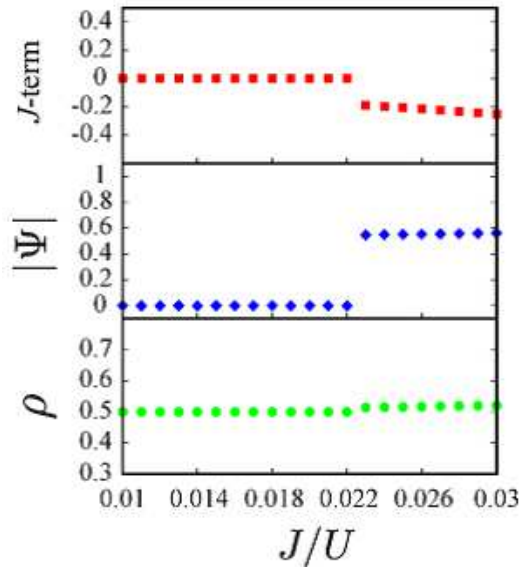


**Figure 2.** Physical quantities in the DW and SF critical region in various system sizes; the hopping  $J$ -term energy, amplitude of SF order ( $|\Psi|$ ), and mean density ( $\rho$ ). The obtained results show that the phase transition is of first order as dictated by Landau-Ginzburg-Wilson paradigm. Critical point is estimated as  $J_c/U \approx 0.022$ .

system exists near the half filling  $\rho \approx 1/2$ , and a first-order phase transition between the DW and SF takes place at  $J_c/U \simeq 0.022$  as a finite jump in  $|\Psi|$  indicates. The existence of the first-order phase transition is quite plausible as the DW and SF have both the own long-range order. In recent paper [40], we studied the EBHM for  $V/U = 0.375$  and near the unit filling  $\rho \approx 1$ . There exists a substantially finite region of the SS in addition to the DW and SF. These three phases are separated by two second-order phase transitions. This result is in agreement with the quantum Monte-Carlo study [41].

In the following, we shall study dynamics of the system under “slow quenches”.

To this end, we employ the tGW methods [43, 44, 45, 46, 47, 48, 49]. In the tGW approximation, the Hamiltonian of the EBHM in Eq.(1) is approximated by a single-site Hamiltonian  $H_i$ , which is derived by introducing the expectation value  $\Psi_i = \langle a_i \rangle$ ,

$$\begin{aligned} H_{\text{GW}} &= \sum_i H_i, \\ H_i &= -J \sum_{j \in i\text{NN}} (a_i^\dagger \Psi_j + \text{H.c.}) + \frac{U}{2} n_i (n_i - 1) \\ &\quad + V \sum_{j \in i\text{NN}} n_i \langle n_j \rangle - \mu n_i, \end{aligned} \quad (2)$$

where  $i\text{NN}$  denotes the NN sites of site  $i$ , and Hartree-Fock type approximation has been used for the hopping and NN repulsion. To solve the quantum system  $H_{\text{GW}}$  in Eq.(2), we introduce GW wave function,

$$|\Phi_{\text{GW}}\rangle = \prod_i^{N_s} \left( \sum_{n=0}^{n_c} f_n^i(t) |n\rangle_i \right), \quad \hat{n}_i |n\rangle_i = n |n\rangle_i, \quad (3)$$

where  $n_c$  is the maximum number of particle at each site, and we mostly take  $n_c = 6$  in the present work. Some quantities are calculated with  $n_c = 10$  to verify that  $n_c = 6$  is large enough for the study of the half filling case. See Fig. 3 and Fig. 7. In terms of  $\{f_n^i(t)\}$ , the order parameter of the SF is given as,

$$\Psi_i = \langle a_i \rangle = \sum_{n=1}^{n_c} \sqrt{n} f_{n-1}^{i*} f_n^i, \quad (4)$$

and  $\{f_n^i(t)\}$  are determined by solving the following Schrödinger equation for various initial states,

$$i\hbar \partial_t |\Phi_{\text{GW}}\rangle = H_{\text{GW}}(t) |\Phi_{\text{GW}}\rangle. \quad (5)$$

The time dependence of  $H_{\text{GW}}(t)$  in Eq.(5) comes from the quench  $J \rightarrow J(t)$  with fixed  $U$  and  $V$  as explained in the following section. Practically, the time evolution above is calculated by the fourth-order Runge-Kutta method.

### 3. Dynamics of phase transition from density wave to superfluid

We first study the dynamics from the DW to SF. In this section, the hopping amplitude is varied as

$$\frac{J(t) - J_c}{J_c} \equiv \epsilon(t) = \frac{t}{\tau_Q}, \quad (6)$$

where  $\tau_Q$  is the quench time, which is a controllable parameter in experiments. We employed 10 samples as the initial state at  $t = -\tau_Q$  (i.e.,  $J(-\tau_Q) = 0$ ), which have the DW order with small local density fluctuations from the perfect DW. Then, we solve Eq.(5) to obtain  $|\Phi_{\text{GW}}\rangle$ . Physical quantities for which scaling laws are examined are obtained by averaging over samples. The linear quench in Eq.(6) is terminated at  $t = t_f$

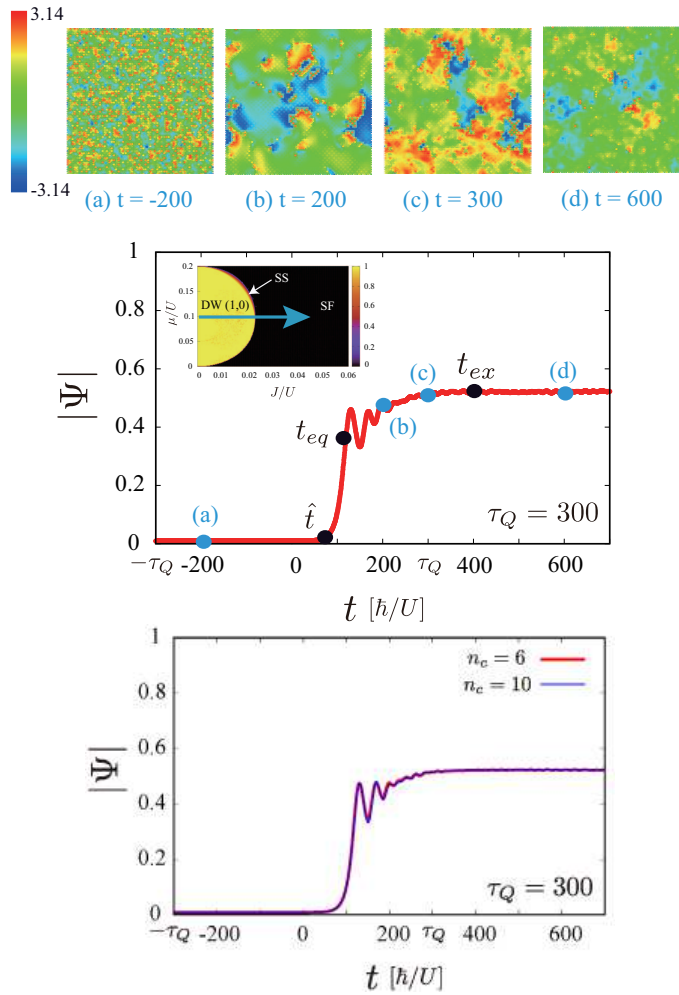


**Figure 3.** (Upper panel) Phase of the SF order parameter  $\Psi_i$  for  $\tau_Q = 300$  as a function of time. (Middle panel) Amplitude of the SF order parameter  $\Psi_i$  for  $\tau_Q = 300$  as a function of time. Relevant times  $\hat{t}$  and  $t_{eq}$  are  $\hat{t} \approx 70$  and  $t_{eq} \approx 120$ , respectively. On the other hand,  $t_{ex} \approx 400$ , at which the oscillation of  $|\Psi|$  terminates. From  $t_{eq}$  to  $t_{ex}$ , coarsening process of the phase of  $\Psi_i$  takes place in large scales [26]. (Lower panel) Calculation of  $|\Psi|$  in the  $n_c = 10$  case is also shown. It is in good agreement with that of  $n_c = 6$ .

with  $J(t_f) = 0.044 (> J_c)$  in the numerical study. Subsequent behavior of the system is also observed to see how the system approaches to an equilibrium.

We show the typical behavior of  $|\Psi|$  as a function of  $t$  in Fig. 3 for  $\tau_Q = 300$ . At  $t = 0$ , the system crosses the critical point at  $J_c/U \simeq 0.022$ . After crossing the critical point,  $|\Psi|$  remains vanishingly small for some period, and then it develops very rapidly. After the rapid increase,  $|\Psi|$  starts to fluctuate and coarsening of the phase of the SF order parameter takes place there [26].  $\hat{t}$  in Fig. 3 is defined as  $|\Psi(\hat{t})| = 2|\Psi(0)|$ , and  $t_{eq}$  is the time at which the oscillation of  $|\Psi|$  starts. Similarly,  $t_{ex}$  is the time at which that oscillation terminates.

Similar behavior to the above was observed in the Mott to SF quench dynamics and

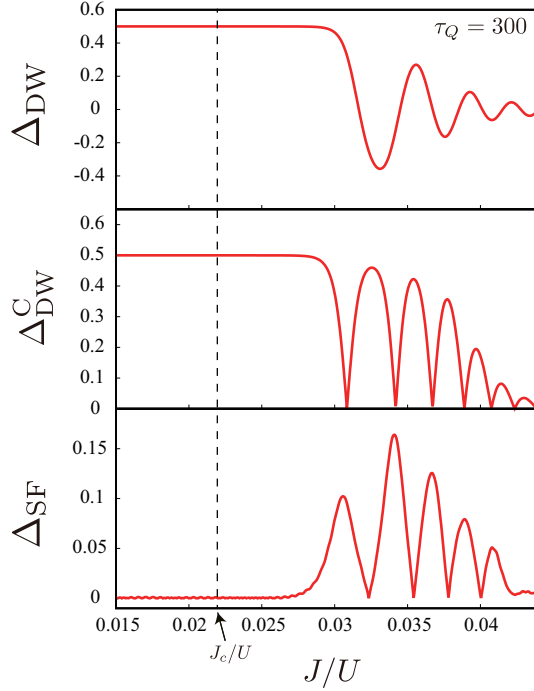


**Figure 4.**  $\Delta_{\text{DW}}$ ,  $\Delta_{\text{DW}}^{\text{C}}$  and  $\Delta_{\text{SF}}$  as a function of time for  $\tau_{\text{Q}} = 300$ . After passing the equilibrium critical point  $J_c/U \simeq 0.022$ , the both quantities start to evolve with oscillations.

examined carefully [26]. Compared with the Mott to SF dynamics, the SF amplitude  $|\Psi|$  is smaller, e.g., for  $t > t_{\text{eq}}$ ,  $|\Psi| \sim (0.8 - 0.9)$  in the Mott to SF transition, whereas  $|\Psi| \sim 0.5$  in the present case. This difference simply comes from the difference of the mean particle density, i.e.,  $\rho \sim 1$  in the Mott to SF transition case.

The DW order parameters  $\Delta_{\text{DW}} \equiv \frac{1}{N_s} \sum_i (-)^i \langle n_i \rangle$ ,  $\Delta_{\text{DW}}^{\text{C}} \equiv \frac{1}{2N_s} \sum_{\langle i,j \rangle} |\langle (n_i - n_j) \rangle|$ , and the even-odd difference of the SF order parameter defined as  $\Delta_{\text{SF}} \equiv \frac{1}{2N_s} \sum_{\langle i,j \rangle} ||\Psi_i| - |\Psi_j||$  are shown in Fig. 4. These quantities exhibit fluctuations as a function of time until  $J \approx 0.045$ . These fluctuations are getting smaller, i.e., the system is approaching to a homogeneous SF. The system with other values of  $\tau_{\text{Q}}$  exhibits a similar behavior, although the reaction of the system starts at larger value of  $J/U$  for smaller value of the quench time  $\tau_{\text{Q}}$ .

It is interesting to study the correlation length  $\xi$  of the SF order parameter and the vortex density  $N_{\text{v}}$  as a function of the quench time  $\tau_{\text{Q}}$ . These quantities are defined as follows;

$$\begin{aligned}
 \langle \Psi_i^* \Psi_j \rangle &\propto \exp(-|i - j|/\xi), \\
 N_{\text{v}} &= \sum_i |\Omega_i|, \\
 \Omega_i &= \frac{1}{4} \left[ \sin(\theta_{i+\hat{x}} - \theta_i) + \sin(\theta_{i+\hat{x}+\hat{y}} - \theta_{i+\hat{x}}) \right. \\
 &\quad \left. - \sin(\theta_{i+\hat{x}+\hat{y}} - \theta_{i+\hat{y}}) - \sin(\theta_{i+\hat{y}} - \theta_i) \right], \tag{7}
 \end{aligned}$$

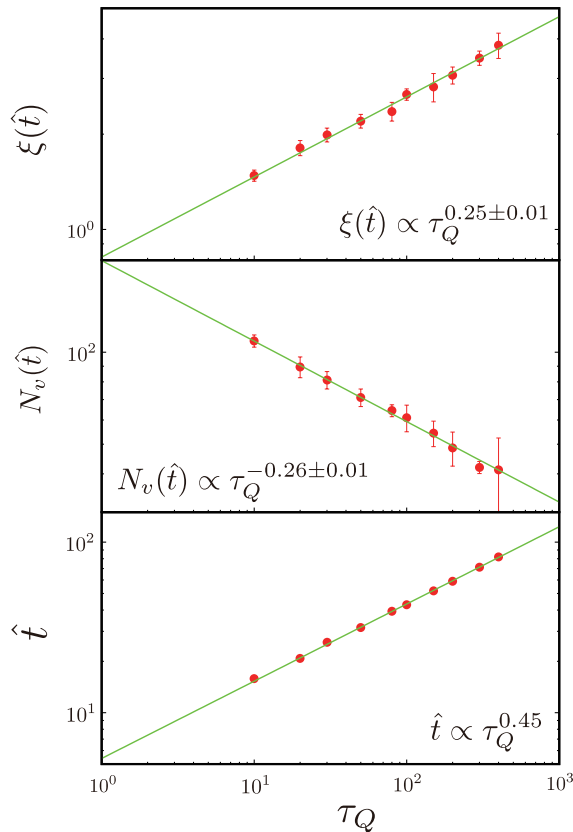


**Figure 5.** Scaling laws observed for the correlation length  $\xi$ , vortex number  $N_v$  at  $t = \hat{t}$ , and  $\hat{t}$  with respect to  $\tau_Q$ .

where  $\theta_i$  is the phase of  $\Psi_i$  ( $\Psi_i = |\Psi_i|e^{i\theta_i}$ ) and  $\hat{x}$  ( $\hat{y}$ ) is the unit vector in the  $x$  ( $y$ ) direction. For continuous second-order phase transitions, the KZ hypothesis predicts a scaling law such as  $\xi \propto \tau_Q^b$  and  $N_v \propto \tau_Q^{-d}$ . Recently, applicability of the above KZ scaling law for *second-order quantum phase transition* has been discussed for several quantum systems. On the other hand for first-order phase transitions, it is commonly expected that such a scaling law does not hold as the relaxation time cannot be defined properly. For a classical statistical model, another type of scaling law was proposed for first-order phase transitions [36]. It should be also noted that off-equilibrium dynamics of a quantum Ising ring was investigated recently and finite-size scaling laws for first-order phase transitions were proposed [37]. There, off-equilibrium scaling variables were given in terms of an energy gap and quench time, and physical quantities were obtained as a function of time.

To see if scaling law exists or not, we measured  $\xi$  and  $N_v$  at  $t = \hat{t}$  and  $t = t_{\text{eq}}$ . In the original KZ hypothesis for continuous phase transitions [11],  $\hat{t}$  is the time at which the system re-enters an equilibrium after the freezing (or impulse) period. On the other hand,  $t_{\text{eq}}$  is the time at which a coarsening process of the SF phase coherence starts [26].

We show the obtained results in Figs. 5 and 6. The results show that at  $t = \hat{t}$ , both  $\xi$  and  $N_v$  satisfy the scaling law with exponents  $b = 0.25$  and  $d = 0.26$ , respectively,



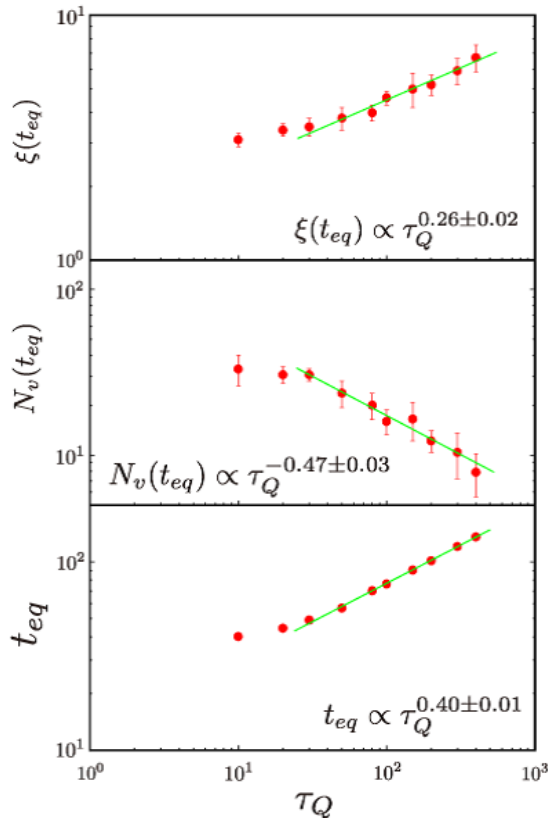


**Figure 6.** Scaling laws observed for the correlation length, vortex number at  $t = t_{eq}$ , and  $t_{eq}$  with respect to  $\tau_Q$ .

and also  $\hat{t} \propto \tau_Q^{0.45}$ . On the other hand at  $t = t_{eq}$ , data at each  $\tau_Q$  exhibits slightly large fluctuations but scaling laws for the correlation length,  $N_v$  and  $t_{eq}$  seem to exist for  $\tau_Q > 20$ . The above results indicate that besides the KZ mechanism, there exists another mechanism to generate the scaling laws. Possible explanation is given in Sec. 4.

It should be noted that after passing the critical point,  $\Delta_{DW}$  and  $\Delta_{SF}$  have even-odd site fluctuations, and therefore, the system is not homogeneous. We think that because of this inhomogeneity, the critical exponents of  $\xi$  and  $N_v$  at  $t = \hat{t}$  do not satisfy the expected relation such as  $b = d/2$ . On the other hand at  $t = t_{eq}$ , the system is rather homogeneous, and therefore  $b \sim d/2$ .

In appendix, we consider the hard-core version of the EBHM and show the calculations of the scaling laws with respect to  $\tau_Q$  in Fig. A.2. There,  $\xi(\hat{t})$  and  $N_v(\hat{t})$  fluctuate rather strongly. This behavior comes from the fact that fluctuations of the particle number at each site is smaller compared with the soft-core case, and as a result, the stability of the phase degrees of freedom of the SF order parameter is weakened.

We terminate the linear quench at  $t_f = \tau_Q = 300$ . After  $t_f$ , the system approaches to an equilibrium as the results in Figs. 3 and 4 indicate. It is interesting to see how the correlation length of the SF develops. As the results in Fig. 7 show, the correlation

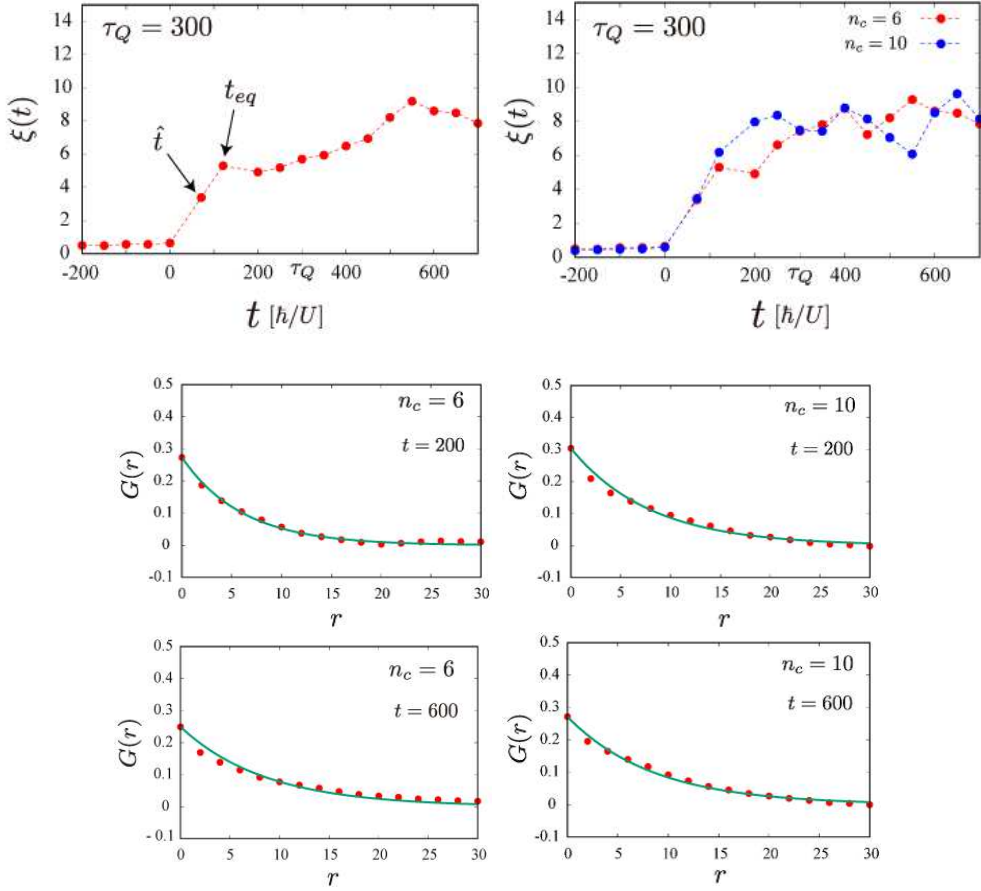


**Figure 7.** (Upper left panel) For a typical initial state at  $t = -\tau_Q$ , the correlation length is calculated as a function of time. After passing  $t = t_{eq}$ , increase of the correlation length becomes weak. (Upper right panel) We also show the results for the  $n_c = 10$  case. (Lower panels) The correlation functions  $G(r) = \frac{1}{2N_s} \sum_i \langle a_i^\dagger a_{i+r} \rangle$  exhibit very close behavior in the  $n_c = 6$  and  $n_c = 10$  cases.

length increases after passing the critical point as it is expected. However, its increase gets weak at  $t \sim t_{eq}$ , and it saturates at  $t \sim 500$  and keeps a finite value. To study the resultant phase, we measured  $N_v$  and found that there exist no vortices at  $t > 500$ . One may expect that the system settles in a *finite-temperature* ( $T$ ) SF phase for sufficiently large  $t$  with an effective  $T$ ,  $T_{eff}$ . The finite- $T$  SF in 2D has a quasi-long range order and the correlation length diverges, i.e., the Kosterlitz-Thouless (KT) phase. The above result seems to indicate that some other state is realized in the final stage of the present process. However, the system behavior may strongly depend on the average particle density  $\rho$ . Further study is needed to clarify this interesting problem. In fact, we studied this problem in the case of the mean particle density  $\rho \approx 1$  and  $V/U = 0.375$  [40]. In the quench process such as the  $DW \rightarrow SS \rightarrow SF$ , the correlation length continues to increase even for large  $t$ . This result seems to indicate that a KT phase of the SF is realized there.

#### 4. Consideration by the Ginzburg-Landau theory

In the previous section, we showed that the results obtained by the GW methods indicate the scaling laws of  $\hat{t}$ ,  $t_{\text{eq}}$  and the correlation length with respect to the quench time  $\tau_Q$ . It is interesting and also important to study the origin of these observations from more universal and intuitive point of view. To this end, the Ginzburg-Landau (GL) theory is quite useful. In fact very recently, it was pointed out that the GL theory can drive the scaling laws for the second-order phase transition by analytical transformation of the associated equations of motion [50]. In this section, we first review the above derivation of the scaling laws for the ordinary second-order phase transition, and then give an intuitive picture of the scaling laws by using a classical solution representing decay of the false vacuum. Then, we extend the methods to the present case involving the SF and DW order parameters. This consideration also gives an insight about the physical meaning and limitation of the GW methods.

##### 4.1. Second-order phase transition

Let us start with the stochastic GL equation for a complex order parameter (condensate)  $\phi(\vec{r}, t)$ ,

$$\frac{\partial \phi}{\partial t} = \nabla_{\vec{r}}^2 \phi - \frac{\epsilon(t)}{2} \phi - \frac{1}{2} |\phi|^2 \phi + \Theta(\vec{r}, t), \quad (8)$$

where  $\Theta(\vec{r}, t)$  represents the uncorrelated white-noise variables with  $\langle \Theta(\vec{r}, t) \Theta(\vec{r}', t') \rangle = T \delta(\vec{r} - \vec{r}') \delta(t - t')$  and  $T$  is the temperature of particles ensemble not participating the Bose-Einstein condensate. As in Ref. [50], we consider the critical parameter  $\epsilon(t)$  such as

$$\epsilon(t) = - \left| \frac{t}{\tau_Q} \right|^\lambda \text{sgn}(t), \quad (9)$$

where  $\lambda$  is a parameter for the quench protocol. Then, let us change variables as follows,

$$\eta = \alpha t, \quad \vec{\ell} = (\alpha)^{1/2} \vec{r}, \quad \tilde{\phi} = \phi / (\alpha)^{1/2}, \quad (10)$$

where  $\alpha = \tau_Q^{-\lambda/(\lambda+1)}$ . In terms of the new variables, the equation of motion (8) leads to

$$\frac{\partial \tilde{\phi}}{\partial \eta} = \nabla_{\vec{\ell}}^2 \tilde{\phi} - \frac{1}{2} |\eta|^\lambda \text{sgn}(\eta) \tilde{\phi} - \frac{1}{2} |\tilde{\phi}|^2 \tilde{\phi} + \frac{1}{\alpha} \Theta(\vec{\ell}, \eta). \quad (11)$$

In Eq.(11), the  $\tau_Q$ -dependence in Eq.(9) disappears except the last white-noise term. From the above fact, it is concluded in Ref. [50] that the  $\tau_Q$ -dependence of  $\hat{t}$  and  $\xi(\hat{t})$  are expected to follow the transformation in Eq.(10), and they are given as follows for sufficiently low  $T$ ,

$$\hat{t} \propto \alpha^{-1} = \tau_Q^{\lambda/(\lambda+1)}, \quad \xi(\hat{t}) \propto \alpha^{-1/2} = \tau_Q^{\lambda/2(\lambda+1)}. \quad (12)$$

For the linear quench  $\lambda = 1$ ,  $\hat{t} \propto \tau_Q^{1/2}$  and  $\xi(\hat{t}) \propto \tau_Q^{1/4}$ . The above estimations agree with those of the KZ scaling with the mean-field exponents such as  $\nu = 1/2$  and  $z = 2$ .

As we show, the above scaling transformation gives an intuitive picture that derives the KZ scaling law. To this end, we put  $\Theta(\vec{r}, t) = 0$  in Eq.(8) and consider a static

potential such as  $\epsilon(t) = -\epsilon_0 < 0$ . In this case, the static ground state is given as  $\phi = \sqrt{\epsilon_0}$ . To study the *sudden quench dynamics*, we consider the decay of the false vacuum  $\phi = 0$  to the true ground state  $\phi = \sqrt{\epsilon_0}$ . In 1D case, a classical solution representing the decay is obtained as follows [39],

$$\phi(t, x) = \sqrt{\epsilon_0} \left[ 1 + \exp \left( \frac{\sqrt{\epsilon_0}}{2} (x - v_0 t) \right) \right]^{-1}, \quad (13)$$

where  $v_0 = \frac{3\sqrt{\epsilon_0}}{2}$ , and  $\phi(t, -\infty) = \sqrt{\epsilon_0}$  and  $\phi(t, \infty) = 0$ . The solution Eq.(13) obviously represents the situation in which the true vacuum  $\phi = \sqrt{\epsilon_0}$  born in the false vacuum expands with the speed  $v_0$ .

Let us consider the ‘‘slow’’ quench dynamics and study bubble nucleation-evolution process in the SF formation. We expect that this process corresponds to the numerical studies in the previous sections. We have to find the solution to Eq.(8) that describes a single SF-bubble evolution in the false vacuum  $\phi = 0$ , but we cannot find an exact solution. However, the above solution in Eq.(13) suggests that a spherically-symmetric solution in higher dimensions and also for the time-dependent  $\epsilon(t)$  has the following form for  $\epsilon(t) < 0$ ,<sup>‡</sup>

$$\phi_s(\vec{r}, t) = \sqrt{|\epsilon(t)|} F \left( \sqrt{|\epsilon(t)|} (r - v_t t) \right), \quad r > 0, \quad (14)$$

where  $v_t = C_0 \sqrt{|\epsilon(t)|}$  with a certain constant  $C_0$ , and  $F(x)$  is a decreasing function such as  $F(-\infty) = 1$  and  $F(\infty) = 0$ . In fact, we can show that the function  $\phi_s(\vec{r}, t)$  in Eq.(14) satisfies the scaling transformation in Eq.(10) for the time-dependent  $\epsilon(t)$  in Eq.(9), i.e.,

$$\tilde{\phi}_s(\eta, \vec{\ell}) = \phi_s / (\alpha)^{1/2} = \sqrt{\eta^\lambda} F \left( \sqrt{\eta^\lambda} (\ell - v(\eta)\eta) \right), \quad v(\eta) = C_0 \sqrt{\eta^\lambda}, \quad (15)$$

does not depend on  $\tau_Q$ . As far as the above picture holds in the time evolution of the system, Eq.(15) implies that typical events and phenomena are observed similarly in systems with various  $\tau_Q$ 's, and corresponding times have  $\tau_Q$ -dependence such as  $\tau_Q^{\lambda/(\lambda+1)}$ . For example, we numerically obtained  $\hat{t}$  and  $t_{\text{eq}}$  for various  $\tau_Q$ 's in Sec. 3 by starting with qualitatively the same initial states. These values are related to  $\tau_Q$ -independent  $\hat{\eta}$  and  $\eta_{\text{eq}}$  that are obtained by the rescaled picture from Eq.(15), i.e.,  $\hat{t}$  and  $t_{\text{eq}}$  in the  $\tau_Q$ -system are given by  $\hat{t} = \tau_Q^{\lambda/(\lambda+1)} \hat{\eta}$  and  $t_{\text{eq}} = \tau_Q^{\lambda/(\lambda+1)} \eta_{\text{eq}}$ .<sup>§</sup> Furthermore, a typical linear size of the bubble at  $t$ , i.e., the correlation length at  $t$ ,  $\xi(t)$ , is given as

$$\xi(t) = \int_0^t v_t dt \propto \frac{1}{\tau_Q^{\lambda/2}} t^{\lambda/2+1}, \quad (16)$$

<sup>‡</sup> Solution in Eq.(14) might be regarded a solution in the slow quench limit, in which the time-derivative of  $\epsilon(t)$  is small. However, it also satisfies the scaling transformation with  $\epsilon(t)$  in Eq.(9). See the discussion below.

<sup>§</sup> Rough estimation of  $\hat{\eta}$  and  $\eta_{\text{eq}}$  are the followings. As  $\hat{t}$  is determined by the condition such as  $|\Psi(\hat{t})| = 2|\Psi(0)|$ ,  $\sqrt{\hat{\eta}^\lambda} (v(\hat{\eta})\hat{\eta})^2 = \text{constant}$  for the 2D case. On the other hand, as  $t_{\text{eq}}$  is the time at which the overlap of SF bubbles starts [26],  $v(\eta_{\text{eq}})\eta_{\text{eq}} = \text{constant}$ . Simulation for various  $\lambda$ 's is a future work.

and therefore,  $\xi(\hat{t}) \propto (\tau_Q)^{\lambda/2(\lambda+1)} \hat{\eta}^{(\lambda+2)/2}$  and  $\xi(t_{\text{eq}}) \propto (\tau_Q)^{\lambda/2(\lambda+1)} \eta_{\text{eq}}^{(\lambda+2)/2}$ . After  $t_{\text{eq}}$ , the merging and coarsening process of SF bubbles takes place [26], and therefore the above picture and also the resultant scaling laws do not hold anymore.

#### 4.2. GL theory, GW methods and quantum Monte-Carlo simulation

Here, it is suitable to comment on the GW approximation. The GL theory and also the Gross-Pitaevskii (GP) equation consider only the mean field and totally ignore fluctuations around it. On the other hand in the GW approximation, we focus on a wave function of site factorization, and wave function at each site is obtained by solving the site-factorized Hamiltonian in which the NN operators are replaced with their expectation values [26]. The uncertainty relation between the particle number and phase at each site is faithfully taken into account although an equation of motion similar to the GL (GP) equation is derived by the GW methods. This is an advantage of the GW approximation over the GL and GP theories.

As more reliable methods, let us consider the quantum Monte-Carlo (MC) simulations of the coherent-state path integral in the imaginary-time formalism. In this MC simulations, quantum operators are reduced into classical variables and the quantum superpositions are treated by the fluctuations in the imaginary-time direction. Large number of configurations are generated by the MC updates and physical quantities are calculated by averaging them over generated configurations. In the Metropolis MC algorithm, the local updates are applied to variables at each site by calculation a local energy around that site. In the vicinity of a phase transition point, a large number of configurations contribute equally, and calculations by large CPU times are required in order to take into account all relevant configurations. On the other hand away from the critical point, the number of important configurations is not so large. From the viewpoint of the MC simulation with the local update, we can get an interesting insight into the GW approximation. That is, let us imagine that we perform a GW calculation for a system with size  $10^4 \times 10^4$ . When we calculate expectation values, we divide the  $10^4 \times 10^4$  system into  $10^4$  number of  $10^2 \times 10^2$  subsystems. We obtain the expectation values by averaging values calculated in each subsystem. Compared with the path-integral MC simulation, this method is more reliable as the uncertainty relation is faithfully respected. [In the path-integral MC simulation, this relates to the problem how accurately effects of the Berry phase are taken into account. See for example, Ref. [51].] However in the vicinity of the phase transition,  $10^4$  configurations are not sufficient to obtain physical quantities closely related to the singularities of the phase transition. The above consideration suggests that the GW methods are a fairly good approximation for calculating physical quantities that are finite even for the critical regime, e.g., finite order parameters. In other words, the estimation of the critical exponents by the GW methods is not reliable even for using very large systems.

The above consideration may over estimate the reliability and applicability of the GW methods, but it explains why the GW methods often succeed in obtaining correct

results such as the phase diagrams, etc. We expect that the GW methods also works for the correlation functions as far as the correlation length is finite as the quantum MC simulations do, although at present there are no ways to verify it in the quench dynamics.

### 4.3. First-order phase transition in vicinity of triple point

As the phase diagram in Fig. 1 shows, the present first-order phase transition is located in the vicinity of the triple point of the DW, SF and SS. The GL theory for the quench dynamics in Sec. 4.1 can be applied to this case with some modification. Besides the SF order parameter, we introduce a coarse-grained real DW order parameter,  $D(\vec{r}, t) [\sim (-)^i n_i]$ . GL equations are given as

$$\frac{\partial \phi}{\partial t} = \nabla_r^2 \phi - \epsilon(t) \phi - g_1 |\phi|^2 \phi - g_3 D^2 \phi, \quad (17)$$

$$\frac{\partial D}{\partial t} = \nabla_r^2 D + m(t) D - g_2 D^3 - 2g_3 D |\phi|^2, \quad (18)$$

where the positive parameters  $g_1, g_2$  and  $g_3$  are phenomenological ones, which are to be determined by the parameters  $U$  and  $V$ . The positivity of  $g_3$  comes from the fact that the SF and DW are competing orders in the original EBHM. On the other hand,  $\epsilon(t)$  and  $m(t)$  are parameters that are determined by  $J(t), U$  and  $V$ . In the quench from the DW to SF, both  $\epsilon(t)$  and  $m(t)$  are decreasing functions of  $t$ .

Let us consider a slow quench, and denote the phase transition time from the DW to SF by  $t_c$ . At  $t = t_c - \delta$  ( $\delta \rightarrow +0$ ), the system is in the DW and then,  $\epsilon(t_c) + g_3 D^2(t_c) = \epsilon(t_c) + \frac{g_3}{g_2} m(t_c) > 0$ ,  $\phi = 0$  and  $D^2 = \frac{m(t_c)}{g_2}$ . On the other hand at  $t = t_c + \delta$  ( $\delta \rightarrow +0$ ), the system is in the SF, and  $m(t_c) - 2g_3 |\phi|^2 = m(t_c) + 2\frac{g_3}{g_1} \epsilon(t_c) < 0$ ,  $|\phi|^2 = -\frac{\epsilon(t_c)}{g_1}$  and  $D = 0$ . From the above equations, we obtain the constraint for the occurrence of the direct DW to SF transition such as  $2g_3^2 > g_1 g_2$ , and  $\epsilon(t_c) < 0$ ,  $m(t_c) > 0$ . The critical time,  $t_c$ , is determined by the condition that the potential energy  $\mathcal{V} = \epsilon(t) |\phi|^2 + \frac{g_1}{2} |\phi|^4 + g_3 D^2 |\phi|^2 - m(t) \frac{D^2}{2} + \frac{g_2}{4} D^4$  has the same value in the DW and SF states at  $t = t_c$ . This condition gives  $\epsilon^2(t_c) = \frac{g_1}{2g_2} m^2(t_c)$ . On the other hand, the triple point is realized by  $\epsilon(t_c) = m(t_c) = 0$  or  $2g_3^2 = g_1 g_2$ .

Let us focus on the SF for  $t \geq t_c$ . In this case,  $D = 0$  and we only consider the GL equation in Eq.(17) with  $D = 0$ . We assume the same protocol with Eq.(9) and then, the transformation in Eq.(12) can be applied as in the case of the second-order phase transition. Correlation length at time  $t$  is estimated as

$$\xi(t) = \int_{t_c}^t v_t dt = \frac{1}{\tau_Q^{\lambda/2}} (t^{\lambda/2+1} - t_c^{\lambda/2+1}). \quad (19)$$

The second term on the RHS in Eq.(19) comes from the finite jump of  $\phi$  at the critical point and indicates the deviation from the genuine second-order phase transition. However for sufficiently small  $t_c$  such as  $t_c \ll \hat{t}, t_{\text{eq}}$ , the correlation length satisfies almost the same scaling law with the KZ one.

## 5. Dynamics of phase transition from superfluid to density wave

This section considers the temporal evolution of the system under a quench from the SF to DW. We found that behaviors of the system strongly depend on the initial state. We shall show the results in the following two subsections.

### 5.1. Evolution from the GW ground-state of SF

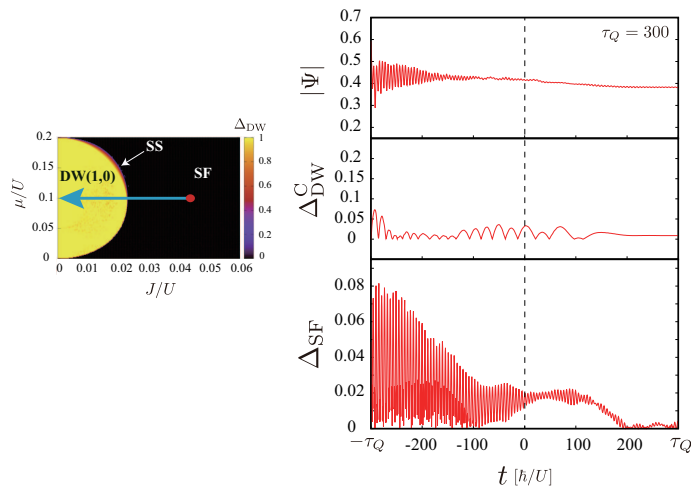


**Figure 8.** Transition from SF to DW with  $J(t_f) = 0$ , Case A. The system passes through the critical point  $J_c$  at  $t = 0$ . Even for  $t > 0$ , both the SF amplitude and DW order parameter do not exhibit the typical behaviors of the DW.

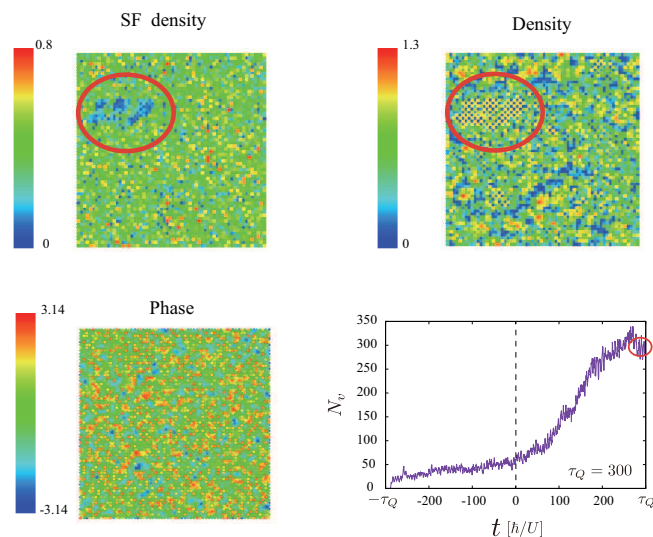


**Figure 9.** Snapshots of SF local density (amplitude), particle density, SF phase degrees of freedom, and vortex density at  $t = \tau_Q$  ( $J/U = 0$ ). Global coherence of  $\Psi_i$  does not exist, and finite-size domains of the DW partially form as indicated by the red circles.

Let us consider the dynamics of the phase transition from the SF to DW. The hopping amplitude is varied as follows in the linear quench,

$$\frac{J_c - J(t)}{J_c} \equiv -\epsilon(t) = \frac{t}{\tau_Q}. \quad (20)$$

In order to clarify the quench dynamics, we shall consider three cases in this subsection. In the first case, Case A, we start with configurations at  $J(t = -\tau_Q) = 2J_c = 0.044$  and terminate the quench at  $t = \tau_Q$  with  $J(\tau_Q) = 0$ . We employ the tGW methods to study the system. In Case A, as well as Cases B and C in the later study in this subsection, *the initial state is the lowest-energy state obtained by the static GW methods.*

The obtained results of  $|\Psi|$ ,  $\Delta_{\text{DW}}$  and  $\Delta_{\text{SF}}$  are shown in Fig. 8 for  $\tau_Q = 300$ .  $|\Psi|$  exhibits fluctuations in the SF for  $t < 0$ , whereas it becomes stable in the region  $J < J_c$  (i.e.,  $t > 0$ ). This behavior comes from the fact that  $\Psi_i$  has a phase coherence in the SF, which induces amplitude fluctuations, as the amplitude and phase of the SF order parameter are quantum conjugate variables with each other. On the other hand in the would-be DW region for  $t > 0$ , the phase coherence is lost, and then the SF amplitude is stable. The DW order parameter  $\Delta_{\text{DW}}$  does not have a stable finite value even after passing through the critical point at  $t = 0$ . These results indicate that some kind of domain structure forms there, i.e., small DW domains may coexist with local SF regions. Calculations of the amplitude of  $\Psi_i$  and the particle density at  $t = \tau_Q$  are shown in Fig. 9. As expected above, DW domains and regions with finite SF amplitude coexist without overlapping with each other.

In Case A, the quench stops with  $J(\tau_Q) = 0$ , and therefore no movement of particles occurs after the quench, and the *particle-density* snapshot in Fig. 9 continues to describe the states for  $t > \tau_Q$ . Similarly, we expect that the coherence of the phase of  $\Psi_i$  is destroyed at  $t = \tau_Q$  because  $J(\tau_Q) = 0$  and also  $\tau_Q = 300$  is a slow quench. See Fig. 9. In order to verify the expected behavior of  $\Psi_i$ , we measured the vortex density as a function of time. At  $t = \tau_Q$ ,  $N_v \sim 300$  is sufficiently large. In summary, in Case A with  $\tau_Q = 300$ , an inhomogeneous state with local DW and SF domains forms after quench. SF order parameter gradually loses its phase coherence during the slow quench.

On the other hand for cases of smaller  $\tau_Q = 100$  and 50, the SF order parameter  $\Psi_i$  is finite even at  $t = \tau_Q$ , and it varies after  $t = \tau_Q$ . The *phase of  $\Psi_i$*  gradually loses its long-range coherence by the existence of the repulsive interactions for  $t > \tau_Q$ .

As Case B, we consider a quench such as  $J(-\tau_Q) = 0.044$  and  $J(0) = J_c = 0.022$  as before but it terminates at  $t = t_f$  with  $J(t_f) = 0.01$ , i.e.,  $t_f = 0.55\tau_Q$  (see Fig. 10). We also study how the system evolves after  $t_f$ . Observed quantities are shown in Fig. 10 for  $\tau_Q = 50$ . The DW order parameter  $\Delta_{\text{DW}}$  develops but its value fluctuates in rather long period after passing  $J_c$  as in Case A. The total energy slightly decreases until  $t_f$ , and the kinetic and on-site energies exhibit fluctuating behavior for  $t < t_f$  although the NN interaction energy is rather stable. This behavior mostly originates from the local density fluctuations, and the stability of the NN interaction comes from the cancellation mechanism between NN sites  $j \in i\text{NN}$ . After passing the critical point at  $t = 0$ , the  $\Psi_i$  keeps a coherent SF order for some period as the calculation of the vortex number



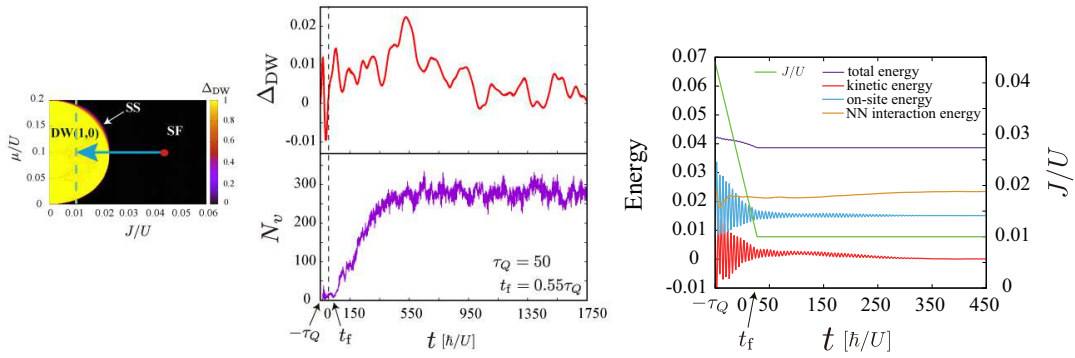


**Figure 10.** Transition from SF to DW with  $J(t_f) = 0.01$ , Case B. Genuine global DW order does not form. After passing  $J_c$  at  $t = 0$ ,  $N_v$  keeps a small value for a while, and the SF order survives there. After passing  $t_f = 0.55\tau_Q = 27.5$ , the total energy of the system keeps a constant value as the system is and isolated one.

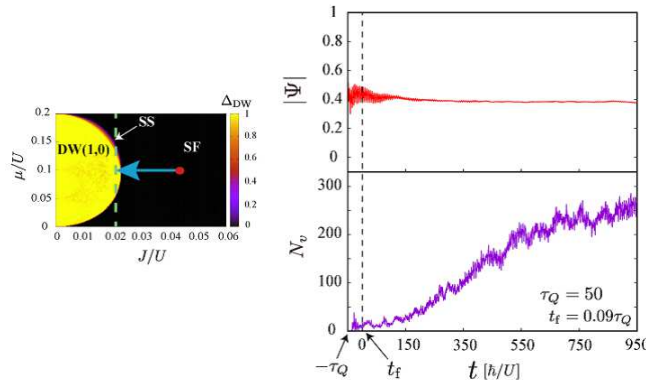


**Figure 11.** Transition from SF to DW with  $J(t_f) = 0.02$ , Case C. Increase of  $N_v$  is slow compared to the cases  $J(t_f) = 0$  and  $J(t_f) = 0.01$ . SF amplitude  $|\Psi|$  also keeps a finite value even for  $t \rightarrow \text{large}$ . However,  $N_v$  increases smoothly, and therefore, the supercooled state formed in the quench is not a meta-stable state.

$N_v$  indicates. At  $t \approx 100$ , it starts to lose the coherence and the SF is destroyed as the increase in  $N_v$  indicates. The state at  $t \sim t_f$  is a *supercooled state*, and a coexisting phase of local domains of the DW and SF is realized there. The observed phenomenon after  $t > t_f$ , therefore, has very similar nature to the *glass transition*, in which the phase coherence and superfluidity are getting lost as the supercooled state evolves after the quench. We call it *quantum glass transition (QGT)* as the hopping amplitude  $J$ , instead of temperature, is the controlled physical quantity and the relevant transition is quantum mechanical one instead of thermal one. We have verified that similar phenomenon is observed for other values of  $\tau_Q$ , e.g.,  $\tau_Q = 20$  and  $200$ .

In both Case A and Case B, the above mentioned QGT is observed *dynamically as a nonequilibrium phenomenon*, i.e., the QGT point is passed through as the system evolves. Therefore as the next problem, it is interesting to see whether there exists a genuine glass transition point,  $J_g (< J_c)$ . Below  $J_g$ , the supercooled state is meta-stable

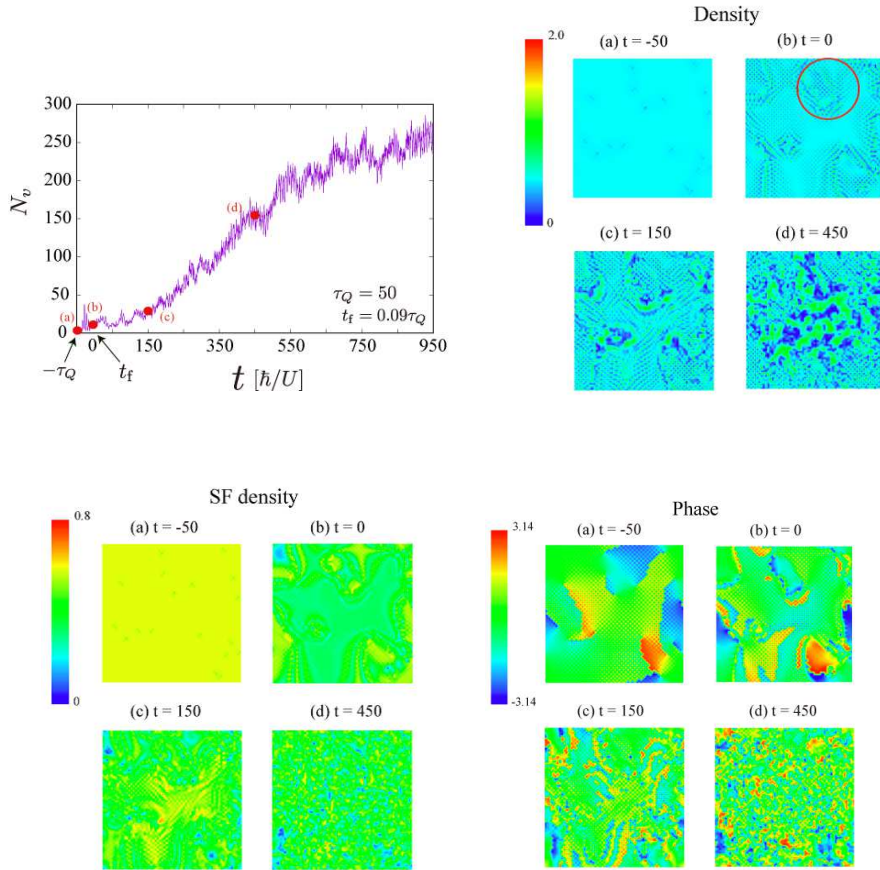


**Figure 12.** (Upper-left) Vortex number as a function of time. Each point denotes the following time; (a)  $t = -50$ , (b)  $t = 0$ , (c)  $t = 150$ , and (d)  $t = 450$ . (Upper-right) Particle density snapshot in Case C. At  $t=0$ , a typical DW domain appears as indicated in the red circle. (Lower-left) SF density snapshot in Case C. (Lower-right) Snapshot of phase degrees of freedom of SF order parameter in Case C.

or at least has a long life time, and the SF survives without losing its phase coherence. For Cases A and B,  $J < J_g$ . Then as Case C, we studied the quench whose final point is  $J(t_f) = 0.02$ , i.e., very close to the equilibrium critical point. Obtained order parameter  $|\Psi|$  and vortex number  $N_v$  are shown in Fig. 11 for  $\tau_Q = 50$ , and time evolution of the particle density, amplitude and phase of  $\Psi_i$  are shown in Fig. 12. After passing the critical point  $J = J_c$  at  $t = 0$ , the domain formation of the DW starts as shown by the particle-density snapshot in Fig. 12, whereas the long-range coherence of the SF order parameter  $\Psi_i$  exists there. Compared with the cases of  $J(t_f) = 0$  and  $J(t_f) = 0.01$ , the destruction of SF and formation of the DW region are slow, but after  $t > 450$ , the quantum glass state forms. Local DW domains develop but also empty regions (voids) form. SF order loses a long-range coherence. This result indicates that  $J_g$  cannot be observed. Similar results are obtained for the case of  $\tau_Q = 20$  and  $\tau_Q = 200$ .

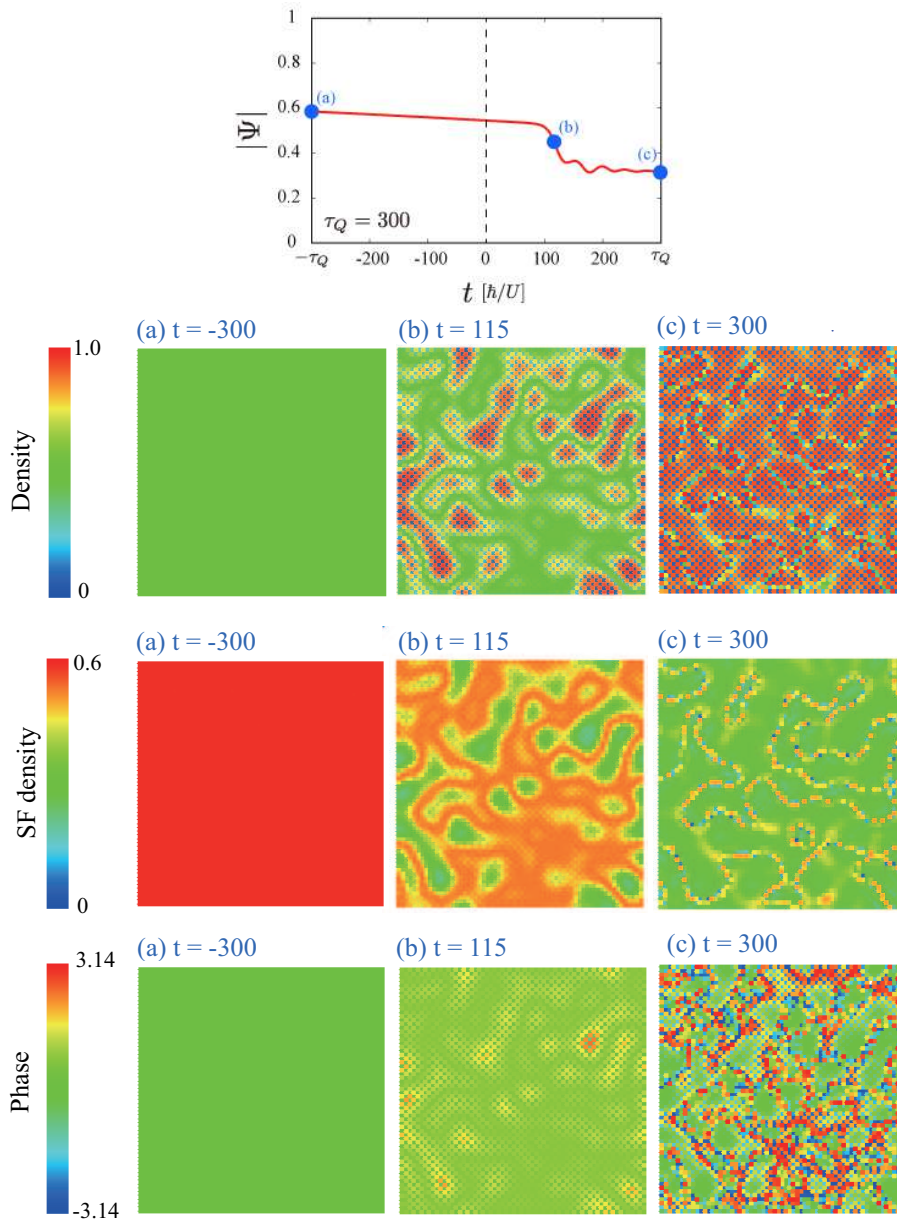


**Figure 13.** (First) SF order parameter as a function of time. Each point denotes the following time; (a)  $t = -300$ , (b)  $t = 115$ , and (c)  $t = 300$ . (Second) Particle density snapshot in Case D. (Third) SF density snapshot in Case D. (Lowest) Snapshot of phase of SF order parameter in Case D. At  $t = 300$ , a large scale DW domain structure with thin domain walls forms. Coherence of SF phase is lost there.

### 5.2. Evolution from SF state with small phase fluctuations

In Sec. 5.1, we studied dynamical evolution of the system from the SF to DW. In that study, the initial state is set to the ground-state obtained by the equilibrium GW methods. It is interesting to see how the dynamical phenomena depend on the initial state as we are considering the first-order phase transition. In order to study this problem, we consider a SF state that is uniform and has almost perfect phase coherence

with very small random fluctuations. For the practical calculation, we employ an initial state GW wave function in Eq.(3) corresponding to  $\Psi_j = \sqrt{\rho}e^{i\delta\theta_j}$  with random numbers  $\{\delta\theta_j\}$  from a uniform distribution  $[-0.005, 0.005] \times \pi$ . The other condition is the same with the Case A, (please refer to the left panel in Fig. 8). We call the present study Case D.

We investigated the time evolution of the system by the tGW methods, and obtained results are shown in Fig. 13. Interestingly enough, the system behavior after passing across the critical point  $J_c$  is substantially different from that in Cases A. The SF order parameter  $|\Psi|$  decreases a finite amount at  $t \sim 100$ , and the density difference at even-odd sublattice increases there. On the other hand, the vortex number starts to increase rapidly at  $t \sim 150$ .

Snapshots of the particle density, SF amplitude and SF phase are shown in Fig. 13. Contrary to Case A, the DW pattern starts to form at  $t \sim 115$  and it develops to the whole system at  $t \sim 300$ , even though there exist domain walls. It should be noticed that a similar behavior was observed for the classical first-order phase transition in Ref. [36]. On the other hand, the SF phase coherence exists at  $t < 115$ , whereas it is destroyed at  $t \sim 300$ .

The initial state of Case D has higher energy than that of Case A. The above numerical result indicates that there exists an energy barrier between the supercooled SF state and the genuine DW, and some amount of energy is need to overcome the barrier. Furthermore, the above result also indicates that the existence of the SF phase coherence in large spatial regions prevents the formation of large size DW domains. In other words, local fluctuations of the superfluidity coherence substantially develops under a quench even if they are initially tiny, and the DW is preferred as a result.

We expect that the above interesting phenomenon is observed by experiments on ultra-cold atomic gases in the near future.

## 6. Conclusion

In this work, we studied dynamical behavior of the EBHM in 2D by using the tGW methods. In the ground-state phase diagram, there are three phases, the SF, DW, and SS. In particular, we are interested in the first-order phase transition between the SF and DW under a slow quench of the hopping amplitude.

First, we investigated the dynamics of the EBHM in the transition from the DW to SF. In the practical calculation, we fix the strength of the one-site and NN repulsions, and vary the hopping parameter  $J$ . After passing through the equilibrium critical point  $J_c$ , the amplitude of the SF order parameter,  $|\Psi|$ , remains vanishingly small until  $t = \hat{t}$ . After  $\hat{t}$ , it develops quite rapidly. Therefore,  $\hat{t}$  has the meaning of the reentry time to the adiabatic region passing from the frozen regime although the present phase transition is of first order. At  $t_{\text{eq}}(> \hat{t})$ ,  $|\Psi|$  starts to oscillate until  $t = t_{\text{ex}}$ . This behavior is quite similar to that in the second-order phase transition from the Mott insulator to SF, which we observed in the previous work [26]. Then we are interested in whether some kind

of scaling laws between the correlation length/vortex number and the quench time  $\tau_Q$  exist. Our numerical study shows that the scaling laws such as  $\xi \propto \tau_Q^b$  and  $N_v \propto \tau_Q^{-d}$  in fact hold. This result is against to the simple expectation that such scaling laws do not exist in the first-order phase transitions because the simple relaxation-time picture and the concept of the (dynamical) critical exponents are not applicable. From this result, we think that there exists another mechanism, besides the KZ mechanism, to generate the scaling laws. As a possible explanation, we studied the present system by using the GL-type theory suggested by Ref. [50]. This consideration indicates that the observed scaling laws come from the fact that the present phase transition point is located in the vicinity of the triple point.

In the second half, we studied the dynamics of the EBHM in the quench of the opposite direction, i.e., from the SF to DW. We focused on how the final value of the hopping amplitude of the quench,  $J(t_f)$ , influences the dynamics of the system during and after the quench.

Our numerical study showed very interesting phenomena. First, in the case for the GW ground-state as the initial state, the genuine DW state does not form even for very slow quench  $\tau_Q = 300$ . Instead, the coexisting state composed of DW and SF domains appears and spatially inhomogeneous structure of that state is stable after the quench. In cases with  $J(t_f) > 0$ , the SF order parameter has a phase coherence at  $t = t_f$ , and after the quench, the SF order is getting weak by the generation of vortices. Obviously, the quench produces a *supercooled state* in which the domain structure of the DW and SF local (i.e., short-range) coherent state forms. These two domains have an off-set structure with each other. Then, after termination of the quench, the SF is destroyed. This phenomenon is a reminiscent of the glass transition in classical polymers etc, and we call the observed phenomenon quantum glass transition.

On the other hand, if we start with the uniform SF state with tiny fluctuations in the phase of the SF order, the system evolves into the DW with thin domain walls.

In the phase diagram of the EBHM near the half-filling shown in Fig. 1, there is the SS phase, and the SS has two phase boundaries with the DW and SF. In the case of the mean particle density  $\rho = 1$  and strong NN repulsion, the region of the SS is large and two second-order phase transitions are observed clearly from the SS to the DW and SF, respectively. It is interesting to study the dynamics in that region, that is, how the system develops crossing through two second-order phase boundaries. Some related problem was recently studied in classical systems, and a modified KZ scaling law was proposed [52]. We studied the above problem in the EBHM by using tGW methods, and results are published in Ref. [40].

## Appendix A. Hard-core Bose-Hubbard model

In this work, we study the EBHM of the soft-core boson. Hard-core extended Bose-Hubbard model (HCEBHM) is also an interesting model and its relationship to the  $s = 1/2$  quantum spin model is often discussed. Hamiltonian of the HCEBHM on the

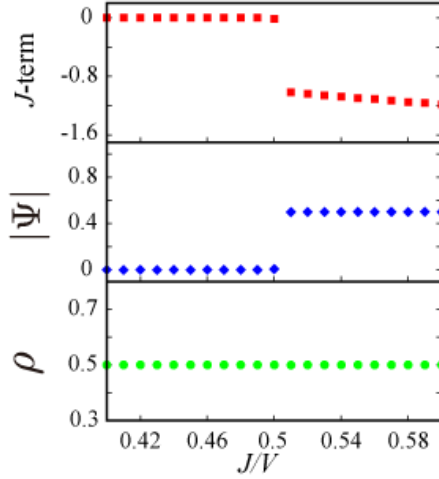


**Figure A.1.** Equilibrium physical quantities obtained by the GW methods.  $\rho = 1/2$  and  $V = 1$ . The results show the existence of a first-order phase transition as the quantum simulations in Refs. [53, 54] proved.

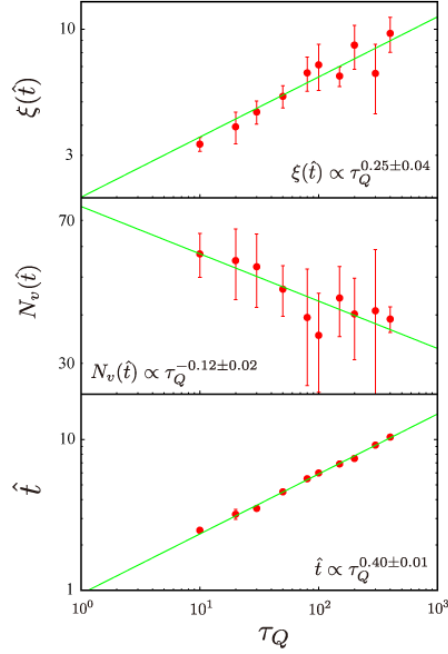


**Figure A.2.** Quench dynamics of the HCEBHM with  $\rho = 1/2$  and  $\tau_Q = 300$ . The correlation length  $\xi$  and vortex density  $N_v$  fluctuate rather strongly compared to the soft-core cases. This result comes from the fact that particle-number fluctuation at each site is restricted by the hard-core constraint, and as a result, fluctuation in the phase of the SF order parameter  $\Psi_i$  is getting large.

square lattice is given as

$$H_{\text{HC}} = -J \sum_{\langle i,j \rangle} (a_i^\dagger a_j + \text{H.c.}) + V \sum_{\langle i,j \rangle} n_i n_j - \mu \sum_i n_i, \quad (\text{A.1})$$

where the on-site interaction terms do not exist by the hard-core nature. Phase diagram of the model in Eq.(A.1) was studied by the quantum MC simulations [53, 54], and it was verified that a first-order phase transition between the DW and SF exists at half filling  $\rho = 1/2$  as in the soft-core case. Then, it is interesting to study the quench dynamics of the HCEBHM by the GW methods.

In this appendix, we shall give numerical calculations of the physical quantities concerning to the static properties of the model in Fig. A.1, and also the  $\tau_Q$ -dependence of  $\hat{t}$ , etc in the quench dynamics in Fig. A.2. The results in Fig. A.1 obviously show that there is a first-order phase transition from the DW to SF for increasing  $J/V$  as the quantum MC simulations in Ref. [53, 54] proved. On the other hand, the correlation length  $\xi$  and vortex density  $N_v$  fluctuate rather strongly compared to the soft-core cases. This result comes from the fact that the HCEBHM has a small fluctuations in the particle number at each site, and as a result, the phase of the SF order parameter fluctuates rather randomly.

## Acknowledgments

Y. K. acknowledges the support of a Grant-in-Aid for JSPS Fellows (No.17J00486).

## References

- [1] Bakr W S ,Gillen J I, Peng A, Folling S and Greiner M 2009 Nature (London) **462** 74
- [2] Georgescu I M, Ashhab S and Nori F 2014 Rev. Mod. Phys. **86** 153
- [3] Cirac J I and Zoller P 2012 Nat. Phys. **8** 264
- [4] Bloch I, Dalibard J and Zwerger W 2008 Rev. Mod. Phys. **80** 885
- [5] Lewenstein M, Sanpera A and Ahufinger V 2012 *Ultracold Atoms in Optical Lattices: Simulating Quantum Many-body Systems* (Oxford University Press, Oxford).
- [6] Kibble T W B 1976 J. Phys. A: Math. Gen. **9** 1387
- [7] Kibble T W B 1980 Phys. Rep. **67** 183
- [8] Zurek W H 1985 Nature **317** 505
- [9] Zurek W H 1993 Acta Phys. Pol. B **24** 1301
- [10] Zurek W H 1996 Phys. Rep. **276** 177
- [11] See for example, del Campo A and Zurek W H 2014 Int. J. Mod. Phys. A **29** 1430018
- [12] Navon N, Gaunt A L, Smith R P and Hadzibabic Z 2015 Science **347** 167
- [13] Chomaz L, Corman L, Bienaime T, Desbuquois R, Weitenberg C, Nascimbene S, Beugnon J and Dalibard J 2015 Nature Comm. **6** 6172
- [14] Dziarmaga J 2005 Phys. Rev. Lett. **95** 245701
- [15] Polkovnikov A 2005 Phys. Rev. B **72** 161201(R)
- [16] Zurek W H, Dorner U and Zoller P 2005 Phys. Rev. Lett. **95** 105701
- [17] Schützhold R, Uhlmann M, Xu Y and Fischer U R 2006 Phys. Rev. Lett. **97** 200601
- [18] Uhlmann M, Schützhold R and Fischer U R 2007 Phys. Rev. Lett. **99** 120407
- [19] Bermudez A, Patane D, Amico L and Martin-Delgado M A 2009 Phys. Rev. Lett. **102** 135702
- [20] Bermudez A, Amico L and Martin-Delgado M A 2010 New J. Phys. **12** 055014
- [21] Chandran A, Erez A, Gubser S S and Sondhi S L 2012 Phys. Rev. B **86** 064304
- [22] Dziarmaga J and Zurek W H 2014 Scientific Reports **4** 5950
- [23] Sonner J, del Campo A and Zurek W H 2015 Nature Comm. **6** 7406
- [24] Francuz A, Dziarmaga J, Gardas B and Zurek W H 2016 Phys. Rev. B **93** 075134

- [25] Gardas B, Dziarmaga J and Zurek W H 2017 Phys. Rev. B **95** 104306
- [26] Shimizu K, Kuno Y, Hirano T and Ichinose I 2018 Phys. Rev. A **97** 033626
- [27] Chen D, White M, Borries C and DeMarco B 2011 Phys. Rev. Lett. **106** 235304
- [28] Braun S, Friesdorf M, Hodgman S S, Schreiber M, Ronzheimer J P, Riera A, del Rey M, Bloch I, Eisert J and Schneider U 2015 Proc. Nat. Acad. Sci. USA **112** 3641
- [29] Anquez M, Robbins B A, Bharath H M, Boguslawski M, Hoang T M and Chapman M S 2016 Phys. Rev. Lett. **116** 155301
- [30] Clark L W, Feng L and Chin C 2016 Science **354** 606
- [31] Cui J-M, Huang Y-F, Wang Z-W, Cao D-Y, Wang J, Lv W-M, Luo L, del Campo A, Han Y-J, Li C-F and Guo G-C 2016 Sci. Rep. **6** 33381
- [32] Bernien H, Schwartz S, Keesling A, Levine H, Omran A, Pichler H, Choi S, Zibrov A S, Endres M, Greiner M, Vuletić V and Lukin M D 2017 Nature **551** 579
- [33] Jaksch D, Bruder C, Cirac J I, Gardiner C W and Zoller P 1998 Phys. Rev. Lett. **81** 3108
- [34] Fisher M P A, Weichman P B, Grinstein G and Fisher D S 1989 Phys. Rev. B **40** 546
- [35] Kovrizhin D L, Venkateswara Pai G and Sinha S 2005 Eur. Phys. Lett. **72** 162
- [36] Pelissetto A and Vicari E 2017 Phys. Rev. Lett. **118** 030602
- [37] Pelissetto A, Rossini D and Vicari E 2018 Phys. Rev. B **97** 094414
- [38] Coulamy I B, Saguia A and Sarandy M S 2017 Phys. Rev. E **95** 022127
- [39] Zurek W H, Bettencourt L M A, Dziarmaga J and Antunes N D 2000 Acta. Phys. Polon. B **31** 2937
- [40] Shimizu K, Hirano T, Park J, Kuno Y and Ichinose I 2018 arXiv:1805.05042
- [41] Ohgoe T, Suzuki T and Kawashima N 2012 Phys. Rev. B **86** 054520
- [42] Dutta O, Gajda M, Hauke P, Lewenstein M, Lhmann D -S, Malomed B A, Sowiski T and Zakrzewski J 2015 Rep. Prog. Phys. **78** 66001
- [43] Jaksch D, Venturi V, Cirac J I, Williams C J and Zoller P 2002 Phys. Rev. Lett. **89** 040402
- [44] Zakrzewski J 2005 Phys. Rev. A **71** 043601
- [45] Jreissaty M, Carrasquilla J, Wolf F A and Rigol M 2011 Phys. Rev. A **84** 043610
- [46] Buchhold M, Bissbort U, Will S and Hofstetter W 2011 Phys. Rev. A **84** 023631
- [47] Natu S S, Hazzard K R A and Mueller E J 2011 Phys. Rev. Lett. **106** 125301
- [48] Fehrmann H, Baranov M A, Damski B, Lewenstein M and Santos L 2004 Opt. Commun. **243** 23
- [49] Horiguchi N, Oka T and Aoki H 2009 Journal of Physics: Conference Series **150** 032007
- [50] Nikoghosyan G, Nigmatullin R and Plenio M B 2016 Phys. Rev. Lett. **116** 080601
- [51] Kuno Y, Suzuki K and Ichinose I 2014 Phys. Rev. A **90** 063620
- [52] Zhai L-J, Wang H-Y and Yin S 2018 Phys. Rev. B **97** 134108
- [53] Schmid G, Todo S, Troyer M and Dorneich A 2002 Phys. Rev. Lett. **88** 167208
- [54] Huo X, Cui Y-Y, Wang D and Lv J-P 2017 Phys. REv. B **95** 023613